AGU100 ADVANCING EARTH AND SPACE SCIENCE

Water Resources Research

Key Points:
- Initially suspended fine clay particles within the water column rapidly accumulate within the sediment bed due to hyporheic exchange
- Fine clay particle storage occurs beneath the mobile layer of the sediment bed defined by the extent of bedform scour
- Formation of the fine particle layer results in reductions of bedform celerity, height, and sediment flux while length is unchanged

Supporting Information:
- Supporting Information S1

Correspondence to:
J. Dallmann,
jonathandallmann2020@u.
northwestern.edu

Impacts of Suspended Clay Particle Deposition on Sand-Bed Morphodynamics

J. Dallmann[1] [ID], **C. B. Phillips[2]** [ID], **Y. Teitelbaum[3]**, **N. Sund[4]** [ID], **R. Schumer[4]** [ID], **S. Arnon[3]** [ID], and **A. I. Packman[1]** [ID]

[1]Department of Mechanical Engineering, Northwestern University, Evanston, IL, USA, [2]Department of Civil and Environmental Engineering, Northwestern University, Evanston, IL, USA, [3]Zuckerberg Institute for Water Research, The J. Blaustein Institutes for Desert Research, Ben-Gurion University of the Negev, Beersheba, Israel, [4]Desert Research Institute, Reno, NV, USA

Abstract Fine particles (0.1–100 microns) are ubiquitous within the water column. Observations on the interactions between suspended fine particles and sediment beds remain limited, reducing our ability to understand the interactions and feedbacks between fine particles, morphodynamics, and hyporheic flow. We performed laboratory experiments to explore changes in bedform morphodynamics and hyporheic flow following the progressive addition of kaolinite clay to the water column above a mobile sand bed. We characterized these interactions by taking high-frequency time series measurements of bed topography and freestream clay concentration combined with solute injections and bed sediment cores to characterize subsurface properties. Deposition of initially suspended clay resulted in a decrease of bedform height, celerity, and sediment flux by 14%, 22%, and 29% when 1000 g was accumulated within the bed (equal to clay/sand mass ratio of 0.4% in the bed). The hyporheic exchange flux decreased by almost a factor of 2 for all clay additions, regardless of the amount of clay eventually deposited in the bed. Post experiment sediment cores showed clay accumulation within and below the mobile layer of the bedforms, with the peak concentration occurring at the most frequent bedform scour depth. These results demonstrate the tight coupling between bed sediment morphodynamics, fine particle (clay) deposition, and hyporheic exchange. Suspended and bed load transport rates are diminished by the transfer of suspended load to the sediment via hyporheic exchange. This coupling should be considered when estimating sediment transport rates.

1. Introduction

In rivers, fine particles with a diameter of <100 microns consist of particulate organic carbon, minerals such as clay, algal and bacterial cells, and other contaminants (Drummond et al., 2014, 2018). Natural sources of these fine particles include induced overland flow and erosion, remobilization of fine particles stored in the stream bed, bank erosion, landslides, and other mass failures (Belmont et al., 2011; Mueller & Pitlick, 2013; Owens et al., 2005; Rose et al., 2018; Sekely et al., 2002). Anthropogenic activity, such as mining, agriculture, logging, and urbanization can increase fines within rivers (Karwan et al., 2011; Nelson & Booth, 2002; Vaughan et al., 2017; Wood & Armitage, 1997; Wolman, 1967). Fine particles represent a significant water quality concern (Bilotta & Brazier, 2008) with harmful effects including increased turbidity in pristine waters (Lloyd et al., 1987), decreasing stream productivity (Ryan, 1991), damage to benthic ecological systems (Owens et al., 2005), and hypoxia in coastal systems due to excess nutrients (Ansari, 2005; Paerl & Otten, 2013). In addition, the fate of contaminants are linked to the dynamics of fine particles (Foster & Charlesworth, 1996; Horowitz, 2009; Zhang et al., 2010).

The flow of water into and out of the stream bed (hyporheic exchange), fine particle transport, and deposition are tightly coupled in river systems (Boano et al., 2014; Harvey et al., 2012; Karwan & Saiers, 2012; Packman & Mackay, 2003; Preziosi-Ribero et al., 2020). In the presence of fine particles, hyporheic exchange leads to deposition and filtration of fine particles due to advective pumping and turbulent exchange with the stream bed (Boano et al., 2014; Packman et al., 2000a, 2000b). The accumulation of fines in the bed via filtration, in turn, leads to decreasing hyporheic exchange (Fox et al., 2018; Packman & Mackay, 2003). These fines may be stored there for long periods of time spanning multiple flood events (Drummond et al., 2014; Harvey et al., 2012). Through their role in setting the storage and release times of fine particles, hyporheic exchange and bed sediment transport are important for understanding the long-term fate of contaminants

and waterborne pathogens (Boano et al., 2014; Drummond et al., 2014). Excessive deposition of fines results in the siltation (colmation) of stream beds reducing the transfer of various solutes and particles such as organic carbon and regulating heat transfer (Hartwig & Borchardt, 2015). Siltation is expected to impact the microbial biomass residing within the upper sediment bed (Merill & Tonjes, 2014) and harm the spawning potential of diadromous fish (Chapman, 1988; Greig et al., 2005; Louhi et al., 2011). Reduction in hyporheic exchange negatively impacts these communities, leading to increased instream nutrient content (Feris et al., 2003, 2004, Li et al., 2017).

Clay and fine particles are prevalent across many fluvial and marine systems from coarse-grained mountain streams to estuarine and shallow marine systems. Coupled fine particle and bed morphodynamic interactions are expected to occur in sand bedded rivers, estuaries, near coastal environments, and shallow marine settings. The presence of stationary sand bedforms, such as dunes and ripples, have been shown to greatly increase hyporheic exchange compared to a featureless bed (Elliot & Brooks, 1997; Fox et al., 2018; Thibodeaux & Boyle, 1987; Packman & Mackay, 2003). The addition of active bed sediment transport remains understudied, though mobile bedforms are known to change hyporheic exchange pathways and reduce the rate of nitrogen removal relative to stationary ones (Zheng et al., 2019). In addition, as mobile bedforms alter the patterns of fine particle deposition and remobilization (Boano et al., 2014; Packman et al., 2001; Phillips et al., 2019), understanding how exchange is impacted by sediment transport is necessary for modeling the fate of fine particles in natural systems where mobile bed conditions are common (e.g., floods). For stationary bedforms, even relatively small amounts of fine particles can disrupt hyporheic exchange (Fox et al., 2018; Packman et al., 2000a, 2000b). However, mobile bedforms disrupt the surface clogging layers that develops in stationary beds, leading to no impact on hyporheic exchange with small fine particle additions and lower flow rates (Rehg et al., 2005). It remains unclear though how this process will be impacted under higher concentrations of fine particles or for sustained background concentrations of fines.

High concentrations of suspended fine particles have been observed to impact bed morphodynamics due to modulation of the stream turbulence. Both river field measurements (Smith & McLean, 1977) and laboratory experiments (Wan, 1984) show that the height to wavelength ratio for sandy bedforms tend to become smaller in the presence of large concentrations of suspended clay. Experiments on mixed clay and sand beds and premixed clay and sand slurries reveal complex feedback mechanisms between clay concentration, bedform morphodynamics, and flow structure (Baas & Best, 2002, 2008; Best, 2005). In particular, the turbulent characteristics of the flow are impacted by higher clay concentrations (conc. > 4 g/L), leading to morphodynamic changes (Baas & Best, 2008). This increased turbulence leads to an increase in both bedform height and wavelength for increasing freestream clay concentration (Baas et al., 2011). However, in the more cohesive beds (clay percentage > 13%), winnowing of clay particles produced a segregated bed composed of a mobile sand layer above a mixed clay/sand bed (Baas et al., 2013).

Though the impact of clay on bed morphodynamics under premixed conditions have been well studied, it remains unclear how deposition and accumulation of suspended fine particles may impact sand bed morphodynamics. This mode of interaction is especially relevant in rivers and estuaries, where the introduction of clay and other fine particles is episodic in nature, often covarying with higher flows due to runoff generated during storms. Further, the ecological implications of the human-induced increases in fine particles to rivers can only be inferred without an understanding of how fine particles (clay) introduced to rivers from their catchment may impact bed morphodynamics and hyporheic exchange. This study uses four experiments to explore the role of clay concentration within the water column on mobile bedforms, clay accumulation within the bed, and hyporheic exchange.

2. Methods

2.1. Experimental Methods

We performed four experimental runs for a constant freestream velocity consisting of episodic injections of kaolinite clay leading to water suspensions of varying concentrations. The experiments differed only in the total amount of clay added to the flume and the sequence (i.e., number) of clay injections. The experiments were conducted using an 8.5 m long by 0.2 m wide tilting recirculating flume, equipped with a pump (Baldor Industrial Motors) that recirculated both water and sediment from the endwell (Figure 1a). Each experiment initially consisted of an initially flat clay free mobile sand bed approximately 10 cm thick—250 kg of Flint Silica 12 (US Silica, Ottawa, IL) with a D_{50} of 0.420 mm given by the manufacturer—under a constant flow.
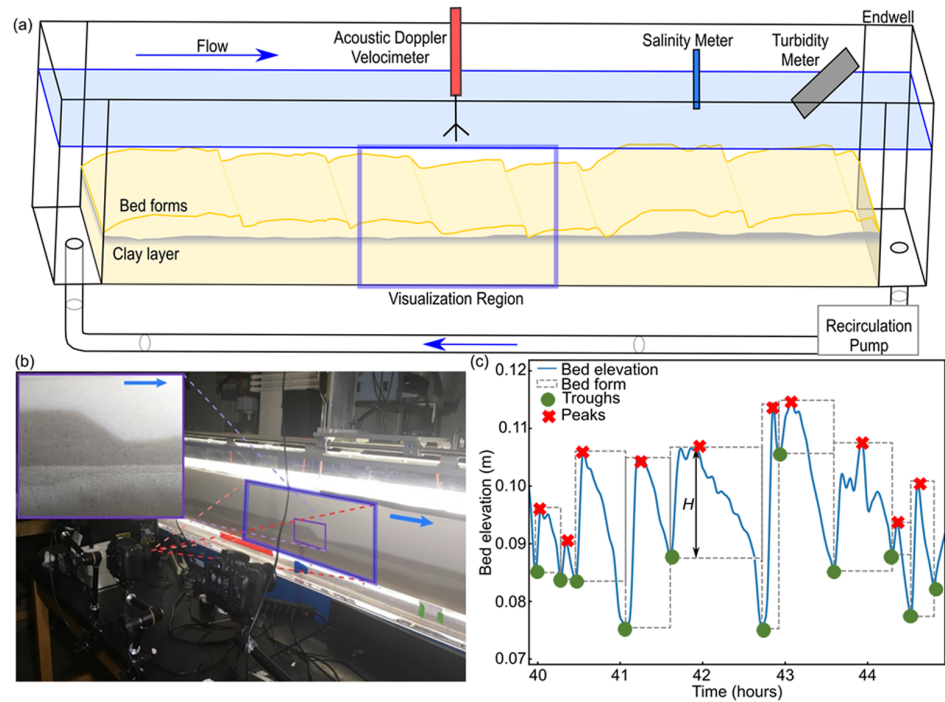
Figure 1. Schematic diagrams of experimental setup and data processing. (a) Schematic of the experimental setup (flow is from left to right). The foreground bedform profile and location of the clay layer represent a partial trace from sidewall images during an experiment. Experimental measurement devices are located in their approximate locations. A porous endplate maintains a minimum sand bed elevation while allowing hyporheic flow to pass. The blue rectangle represents the visualization region of the sidewall camera setup shown in panel (b). (b) Sidewall imaging set up for bedforms following clay injection during Run 3. The blue rectangle represents the FOV of the cameras. The ADV profiler is positioned on a cart directly above the center of the camera FOV. The inset (purple border) shows a close-up of a bedform crest and trough and the accumulation of clay below the mobile layer. (c) Smoothed bedform elevation data from the ADV profiler showing the extracted bedform heights (peak to trough) identified for a portion of Run 1. Note that small bedform ripples (see structure at 44.1 hr) are not treated as individual bedforms.

Mean freestream height (15 cm), mean velocity (0.43 m/s), and shear velocity ($u^* = 0.026$ m/s) were the same for all experiments. The u^* was determined by fitting a log law velocity profile to a time-averaged downstream velocity profile sampled using a Nortek Vectrino Profiler.

The bed was allowed to run for at least a day until mobile bedforms developed and the size distribution reached statistical stationarity. After this developmental period, each experiment consisted of a 4-day clay-free period of sand bed load transport (baseline) followed by one or more clay injections. Baselines were long enough to ensure that enough bedforms were recorded to accurately determine the clay-free average morphodynamic conditions for each run. Relative standard error in measurements of mean bedform height dropped below 5% and 0.4% when 75 and 120 bedforms were measured. We performed four experiments, referred to hereafter as Runs 1–4 (see Table 1 for details). Run 1 consisted of a single clay injection of 1,000 g followed by 261.5 hr of bed elevation measurements. Run 2 consisted of an injection of 333 g every 4 days totaling 277 hr of observations and three injections. Run 3 represented an initial 700 g injection followed by a 300 g clay addition approximately every 1.4 days for the first 300 hr. After 300 hr, the observation time between clay injections was increased. Run 4 consisted of a single initial injection of 5,500 g followed by 256 hr of observation. The injected clay was kaolinite (Snobrite 75, the Cary Company), with a median listed particle diameter of 0.5 μm. For Runs 1–3, the clay was mixed with water matching the flume background salinity (350 μS/cm) in beakers with automatic stirrers for 12 hr prior to the injection. At the background salinity levels, the clay flocculates and the mean D_{50} diameter rises to just above 30 μm. Due to the large amount of clay added, Run 4 was rapidly mixed over a short period (30 min), leading to noticeable amounts of unsuspended clay during the injection. For each injection, the clay was continuously poured into the endwell over the measured recirculation time of the flume (40 s). Following each injection,

Table 1
Information Concerning the Experimental Setup for All Four Runs

	Run 1	Run 2	Run 3	Run 4
Baseline length (hr)	99.5	98	100	100
Post baseline length (hr)	261.5	277	586	256
Number of injections	1	3	17	1
Injection size (g)	1,000	333	300[a]	5,500
Total injected mass (g)	1,000	1,000	5,500	5,500

Note. Each run consists of a baseline without clay after which the first clay injection was conducted. The post baseline period occurs after this first injection. The number of injections (including the initial injection) and the size of each injection are shown.
[a]This run consisted of two closely timed initial injections of 700 and 300 g followed by regular injections of 300 g.

the system was allowed to evolve and changes in the clay concentration, hyporheic exchange, and bedform morphodynamics were observed.

Suspended clay concentration was continuously measured at 1-min intervals with a Xylem turbidity meter (Runs 1 and 2—WTW Visoturb 700IQ SW, Runs 3 and 4 - WTW Visolid 700IQ SW) positioned just upstream of the flume endwell (Figure 1a). Concentration measurements for the first 6.75 hr of Run 1 were taken by hand every hour using a syringe and processed via a spectrophotometer (Hach Company, DR/4000). Because initial instream clay concentrations exceeded the measurement range of the Visoturb 700IQ SW, a calibration curve relating known concentrations of kaolinite to the absorbance of 600 nm light was used to determine the concentration of the samples.

The hyporheic exchange flux (HEF) was measured through salt tracer injections during the baseline and following the end of the experiment. To measure HEF, freestream salinity was recorded following dissolved NaCl tracer injections, typically 10 hr long, using a salinity meter (SM Star Comm, resolution of 0.01 μS/cm). The initial HEF was calculated via regression of the rate of decline in salt concentration with time immediately following the NaCl tracer injection, following the methodology of Fox et al. (2014). No measurement of HEF was performed for the end of Run 4 due to a leak in the flume, which significantly increased the rate of flow into the bed.

Elevation of the sand bed was recorded at a point with an acoustic Doppler velocimeter (ADV) profiler and over a large spatial area with two digital single-lens reflex Nikon D5300 cameras. The ADV was positioned in the center of the camera visualization region located 355 cm from the downstream end of the flume (see Figure 1a). The ADV profiler recorded depth to the sediment bed (2 Hz) from a fixed elevation. Images were taken every minute to visualize bedform propagation and determine bedform length and celerity (see section 2.2, Figure 1b). The cameras were affixed to mounting arms attached to a table adjacent to the flume. They were faced perpendicular to the bed, providing a combined field of view of 180 cm, centered on the profiler and approximately 2.25 times the length of an average bedform. The visualization region was backlit to provide sufficient contrast for automated feature extraction.

At the conclusion of Runs 1–3, 36 cores were taken of the bed following the protocol of Fox et al. (2014) and analyzed for bed clay composition to yield depth averaged clay masses for each 0.5-cm depth interval. In order to extract a core, the flow was stopped, free stream clay was allowed to settle, and the water level was slowly decreased until touching the top of the bed. A syringe was used to remove the settled clay from the surface of the bed by suctioning out the water immediately above the bed in the core measurement region. For two bedforms, three cores were taken, equally spaced in the cross stream direction at six locations: at the downstream trough, at the crest, and at four equally spaced locations between the trough and crest. In total, 18 cores were taken for each bedform sampled. Each core consisted of a 35-ml syringe, 11 cm long by 2.13 cm wide with the tapered end removed. Each core was carefully inserted into the bed, sealed from the bottom, and removed from the flume. Sediments from the cores were extracted in 0.5-cm increments and mixed with 50 ml of deionized water to create a clay suspension. The mixture was weighed and the concentration was determined via absorbance at 600 nm using a spectrometer (Hach Company, DR/4000).

Table 2
Experiment and Bedform Statistics for All Four Runs

Run	t	C_B	H	L	C	Q_t	N	HEF
Base − 1	362	0	0.0227	0.777	0.770	0.00541	146	12.1
Base − 2	379	0	0.0235	0.918	0.904	0.00624	175	12.5
Base − 3	686[a]	0	0.0234	0.865	0.870	0.00603	169	13.5
Base − 4	356	0	0.0223	0.838	1.039	0.00681	156	N/A[b]
Clay − 1	362	322	0.0205	0.730	0.634	0.00400	146	4.6
Clay − 2	379	239	0.0214	0.825	0.835	0.00556	128	4.7
Clay − 3	686[a]	609	0.0209	0.796	0.763	0.00486	132	5.7
Clay − 4	356	990	0.0181	0.805	0.769	0.00442	143	N/A[b]

Note. The total length of the entire run (baseline and post baseline) is given by t and measured in hours. The first four rows represent clay-free baseline data, and the last four represent data taken after clay injection. Each measurement period is 4 days long. For the baseline data, the clay mass in the bed - C_B (g) is 0, while for the clay runs, C_B represents the average clay in the bed over the final 4-day window. H, L, C, and Q_t are averages of bedform height (m), length (m), celerity (m/hr), and sediment flux (m^2/hr) for the initial 96 hr (*Base*) and final 96 hr (*Clay*). N is the number of bedforms measured during each 4-day period as recorded by the ADV profiler. HEF is the hyporheic exchange flux in cm/day.
[a]Time here is the duration of the entire run. Because of a camera data collection failure near the end of the run (see Figure S2 in the supporting information), results in this table were gathered for the contiguous 4-day period preceding the failure (479-575 hr)   [b]Due to a flume leak, it was impossible to obtain final hyporheic exchange data for this run.

These concentrations were subsequently converted into a clay percentage by mass for each depth slice within the core.

2.2. Data Processing

The time series of the bed elevation recorded by the ADV profiler was smoothed using a Savitzky-Golay filter (Python 2.7 SciPy, window size of 509 data points, 255 s) and processed to remove extraneous noise on the elevation signal. A "find peaks" algorithm (Python 2.7 SciPy) was used to identify both the troughs and the peaks of the bed elevation. The height of individual bedforms (H) was defined as the vertical distance between the bedform peak and downstream (lee side) trough (Figure 1c). Small transient ripples, persisting for no more than several minutes with $H < 0.5$ cm, were removed from the time series prior to calculating the final bedform statistics. For each run, Table 2 shows the number of bedforms identified during both the baseline period and the last 4 days of data collection.

Bedform length (L) and celerity (C) were obtained by image analysis of the sidewall camera images. Raw images from each camera were thresholded using a simple black/white thresholding procedure (MATLAB R2019a) that involved using a manually identified black/white pixel cutoff to determine the sediment water interface. The images from both cameras then were stitched together to extract an elevation profile for the full 180-cm field of view, allowing for the simultaneous visualization of multiple bedforms. Increased freestream clay concentration decreased the light exposure requiring manual calibration of the thresholding algorithm following each clay addition. Stitched images were generated, and the black/white pixel cutoff was shifted until the sediment water interface was correctly identified. During data processing, sample images were saved every 100 min to ensure that the interface was correctly identified and that clay deposition didn't alter the camera light exposure. The resultant sidewall bed elevation profile was processed to extract bedform height using the same methods developed for the ADV profiler. Bedform lengths were calculated as the distance between successive troughs, while celerity was calculated as the slope of a linear regression line fit to a trough's downstream location over time. The bedload sediment flux (Q_t) was determined as $Q_t(t) = \beta \psi cH$ (Bagnold, 1941; Martin & Jerolmack, 2013; McElroy & Mohrig, 2009; Simons, 1965) where the bedforms were approximated as triangles with a shape factor $\beta = 0.5$ (Martin & Jerolmack, 2013). The relative proportion of clay within the bed sediment remained low in all experiments, so the porosity was assumed to remain constant for the sand mass flux calculations ($\psi = 0.48$). Average quantities for the baseline and final set of bedforms are provided in Table 2.

DOCKET ALARM

Explore Litigation Insights

Docket Alarm provides insights to develop a more informed litigation strategy and the peace of mind of knowing you're on top of things.

Real-Time Litigation Alerts

Keep your litigation team up-to-date with **real-time alerts** and advanced team management tools built for the enterprise, all while greatly reducing PACER spend.

Our comprehensive service means we can handle Federal, State, and Administrative courts across the country.

Advanced Docket Research

With over 230 million records, Docket Alarm's cloud-native docket research platform finds what other services can't. Coverage includes Federal, State, plus PTAB, TTAB, ITC and NLRB decisions, all in one place.

Identify arguments that have been successful in the past with full text, pinpoint searching. Link to case law cited within any court document via Fastcase.

Analytics At Your Fingertips

Learn what happened the last time a particular judge, opposing counsel or company faced cases similar to yours.

Advanced out-of-the-box PTAB and TTAB analytics are always at your fingertips.

API

Docket Alarm offers a powerful API (application programming interface) to developers that want to integrate case filings into their apps.

LAW FIRMS

Build custom dashboards for your attorneys and clients with live data direct from the court.

Automate many repetitive legal tasks like conflict checks, document management, and marketing.

FINANCIAL INSTITUTIONS

Litigation and bankruptcy checks for companies and debtors.

E-DISCOVERY AND LEGAL VENDORS

Sync your system to PACER to automate legal marketing.

fastcase®
Smarter legal research.